Precision Determination of the Small-x Gluon from Charm Production at LHCb

Rhorry Gauld[1,2,*] and Juan Rojo[3,4,†]
[1]Institute for Theoretical Physics, ETH, CH-8093 Zurich, Switzerland
[2]Institute for Particle Physics Phenomenology, University of Durham, DH1 3LE Durham, United Kingdom
[3]Department of Physics and Astronomy, VU University Amsterdam, De Boelelaan 1081, NL-1081 HV Amsterdam, The Netherlands
[4]Nikhef, Science Park 105, NL-1098 XG Amsterdam, The Netherlands

(Received 4 November 2016; revised manuscript received 14 December 2016; published 15 February 2017)

The small-x gluon in global fits of parton distributions is affected by large uncertainties from the lack of direct experimental constraints. In this Letter, we provide a precision determination of the small-x gluon from the exploitation of forward charm production data provided by LHCb for three different center-of-mass (c.m.) energies: 5 TeV, 7 TeV, and 13 TeV. The LHCb measurements are included in the parton distribution function (PDF) fit by means of normalized distributions and cross-section ratios between data taken at different c.m. values, $R_{13/7}$ and $R_{13/5}$. We demonstrate that forward charm production leads to a reduction of the PDF uncertainties of the gluon down to $x \simeq 10^{-6}$ by up to an order of magnitude, with implications for high-energy colliders, cosmic ray physics, and neutrino astronomy.

DOI: 10.1103/PhysRevLett.118.072001

The determination of the internal structure of the proton, as encoded by the nonperturbative parton distribution functions (PDFs) [1–3], has far-reaching implications for many areas in nuclear, particle, and astroparticle physics. A topic that has recently attracted substantial interest is the determination of the gluon PDF at small x, which is of direct relevance for the modeling of soft QCD at the LHC [4], neutrino astronomy [5–8], and cosmic ray physics [9], as well as for future lepton-proton [10] and proton-proton higher-energy colliders [11]. Constraints on the gluon PDF from deep-inelastic scattering inclusive and charm structure functions at HERA [12,13] are limited to $x \gtrsim 3 \times 10^{-5}$ in the perturbative region, and, consequently, for smaller values of x there are large uncertainties resulting from the lack of direct experimental information.

In 2015, it was realized [14–16] that a way forward was provided by considering inclusive D meson production in pp collisions at the LHC, for which the LHCb experiment had already provided data at 7 TeV [17]. The inclusive charm cross section at the LHC is dominated by heavy quark pair production, in turn driven by the gluon-gluon luminosity, and the forward LHCb kinematics allow a coverage of the small-x region that can reach as low as $x \simeq 10^{-6}$. While the direct inclusion of absolute D meson cross sections into a PDF fit is unfeasible due to the large theory uncertainties that affect the NLO calculation, it has been demonstrated [14,15] that, by using tailored normalized distributions, it is possible to exploit the LHCb measurements to achieve a significantly improved description of the small-x gluon. A complementary approach, suggested in Ref. [16], would be to include D meson data in PDF fits with the use of ratios of cross sections between different center-of-mass (c.m.) energies, which benefit from various uncertainty cancellations [18].

More recently, the LHCb Collaboration presented the analogous D meson cross-section measurements at $\sqrt{s} = 5$ and 13 TeV [19–21], together with the corresponding ratios $R_{13/7}$ and $R_{13/5}$. In this Letter, we quantify the impact of the LHCb D meson data at different c.m. energies on the small-x gluon from the NNPDF3.0 global analysis [22]. These data are included both in terms of normalized cross sections and by means of the cross-section ratio measurements. Our strategy leads to a precise determination of the small-x gluon, substantially improving upon previous results and highlighting the consistency of the LHCb measurements at the three c.m. energies. We illustrate the implications of our results for ultra-high-energy (UHE) neutrino-nucleus cross sections $\sigma_{\nu N}(E_\nu)$, and the longitudinal structure function $F_L(x, Q^2)$ at future lepton-proton colliders.

The LHCb D meson production data are presented double differentially in transverse momentum (p_T^D) and rapidity (y^D) for a number of final states, D^0, D^+, D_s^+, and D^{*+}, which also contain the contribution from charge-conjugate states. To include these measurements in the global PDF fit, we define two observables,

$$N_X^{ij} = \frac{d^2\sigma(X\text{TeV})}{dy_i^D d(p_T^D)_j} \Big/ \frac{d^2\sigma(X\text{TeV})}{dy_{\text{ref}}^D d(p_T^D)_j}, \tag{1}$$

$$R_{13/X}^{ij} = \frac{d^2\sigma(13\ \text{TeV})}{dy_i^D d(p_T^D)_j} \Big/ \frac{d^2\sigma(X\text{TeV})}{dy_{\text{i}}^D d(p_T^D)_j}, \tag{2}$$

which benefit from the partial cancellation of the residual scale dependence from missing higher orders while retaining sensitivity to the gluon since different regions of x are probed in the numerator and the denominator of these observables. The ratio measurements, $R_{13/7}$ and $R_{13/5}$, are

 © 2017 American Physical Society

available for $y^D \in [2.0, 4.5]$ in five bins and for $p_T^D \in [0, 8]$ GeV in eight bins. The 5 and 13 TeV absolute cross-section measurements extend to higher p_T^D values; however, these additional points are excluded from the fit since they might be affected by large logarithmic contributions [23]. The reference rapidity bin in the normalized distributions N_X^{ij} in Eq. (1) is chosen to be $y_{\rm ref}^D \in [3.0, 3.5]$, as in Ref. [15], since we have verified that this choice maximizes the cancellation of scale uncertainties for the considered data. We restrict our analysis to the $\{D^0, D^+, D_s^+\}$ final states, except for 7 TeV, where the D_s^+ data, with large uncertainties, are not considered.

The theoretical predictions for D meson production are computed at next-to-leading order plus parton shower (NLO + PS) accuracy using POWHEG [24–26] to match the fixed-order calculation [27] to the Pythia8 shower [28,29] with the MONASH 2013 tune [4]. The POWHEG results were previously shown to be consistent [14,30] with both the NLO + PS (a) MC@NLO [31,32] method and the semi-analytic FONLL calculation [33,34]. The NNPDF3.0 NLO set of parton distributions with $\alpha_s(m_Z) = 0.118$, $N_f = 5$ and $N_{\rm rep} = 1000$ replicas has been used, interfaced with LHAPDF6 [35]. The internal POWHEG routines have been modified to extract α_s from LHAPDF6, and the compensation terms [33] to consistently match the $N_f = 5$ PDFs with the fixed-order $N_f = 3$ calculation [27] are included. The central value for the charm quark pole mass is taken to be $m_c = 1.5$ GeV, following the HXSWG recommendation [36], and the renormalization and factorization scales are set equal to the heavy quark transverse mass in the Born configuration, $\mu = \mu_R = \mu_F = \sqrt{m_c^2 + p_T^2}$.

Other settings of the theory calculation, such as the values for fragmentation fractions, are the same as those in Ref. [14]. We have verified that the choice of Pythia8 tune (comparing MONASH 2013 with 4C or A14) as well as the modeling of the charm fragmentation (using, for example, a Peterson function with $\epsilon_D = 0.05$ and varying ϵ_D by a factor of 2) on the observables of Eq. (1) leads, in all cases, to variations that are negligible compared to the PDF uncertainties.

The impact of the LHCb D meson data on the NNPDF3.0 small-x gluon can be quantified using the Bayesian reweighting technique [37,38]. We have studied separately the impact of the three data sets of normalized distributions, N_5, N_7, and N_{13}, and the two cross-section ratios, $R_{13/5}$ and $R_{13/7}$, as well specific combinations of these, always avoiding double counting. The experimental bin-by-bin correlation matrices are included for the cross-section ratios $R_{13/X}$, while, for the normalized cross-section data, where the experimental correlation matrix is only available for N_5 and N_{13}, statistical and systematic uncertainties are added in quadrature.

We find that, while NLO theory describes successfully the cross-section ratios $R_{13/7}$ and $R_{13/5}$ and the majority of the data points that compose the normalized distributions N_5, N_7, and N_{13}, poorer agreement is found for a number of points in the D^0 final state at both 5 and 13 TeV, particularly for those which are farthest from the reference rapidity bin $y_{\rm ref}^D$. Note also that the D^0 final state is the one that exhibits the smallest experimental uncertainties. This may indicate the need for the full next-to-next-to-leading order (NNLO) calculation, thus far available only for $t\bar{t}$ production [39]. To avoid this problem, for the N_5 and N_{13} D^0 final state, we impose kinematic cuts and restrict the fitted data set to those points in neighboring rapidity bins of $y_{\rm ref}^D$. We have verified (see Fig. 3) that our results are stable with respect to the specific choice of $y_{\rm ref}^D$.

To illustrate the good agreement found for the considered LHCb data and the corresponding NLO theory predictions, we compute the $\chi^2/N_{\rm dat}$ for each of the five data sets, for different combinations of data used as inputs in the PDF fit. These results are summarized in Table I, where the data that have been included in each case are highlighted in boldface, and the number in brackets indicates $N_{\rm dat}$ for each data set. For example, the first row corresponds to the baseline PDF set, the second row indicates the resultant $\chi^2/N_{\rm dat}$ for each data set after the N_5 data have been added to NNPDF3.0, and so on.

We find that the normalized distributions, N_5, N_7, and N_{13}, as well as the ratio $R_{13/5}$, have a similar substantial pull on the gluon, both for central values and for the reduction of the PDF uncertainty. The $R_{13/7}$ ratio pulls the small-x gluon in the same direction, but with less constraining power. We find it reassuring that including each of the five available LHCb data sets to NNPDF3.0, one at a time, improves the description of all other data sets. In Fig. 1 we show the 1σ relative PDF uncertainties for the gluon at $Q^2 = 4$ GeV^2 in NNPDF3.0 and in the subsequent fits when the various LHCb D meson data sets are included.

In the following, we show results for two representative combinations of the LHCb measurements, namely, $N_7 + R_{13/5}$ and $N_5 + N_7 + N_{13}$. In Fig. 2, we compare the small-x gluon in NNPDF3.0 with the resultant gluon in these two cases, as well as the central value from the $N^5 + R^{13/7}$ fit. The central value of the small-x gluon is

TABLE I. The $\chi^2/N_{\rm dat}$ for the LHCb D meson measurements considered, N_5, N_7, N_{13}, $R_{13/7}$, and $R_{13/5}$, for various combinations of input to the PDF fit (highlighted in boldface).

$N_5(70)$	$N_7(59)$	$N_{13}(106)$	$R_{13/5}(107)$	$R_{13/7}(75)$
1.81	1.16	1.79	1.53	0.97
1.01	0.65	0.92	1.48	0.95
1.47	**0.89**	1.34	1.50	0.94
1.09	0.68	**0.97**	1.49	0.94
1.15	0.73	1.09	**1.41**	0.96
1.44	0.87	1.30	1.46	**0.93**
1.05	0.67	0.95	1.48	**0.95**
0.98	**0.64**	0.91	**1.45**	0.96
1.14	**0.7**	**1.01**	1.49	0.94

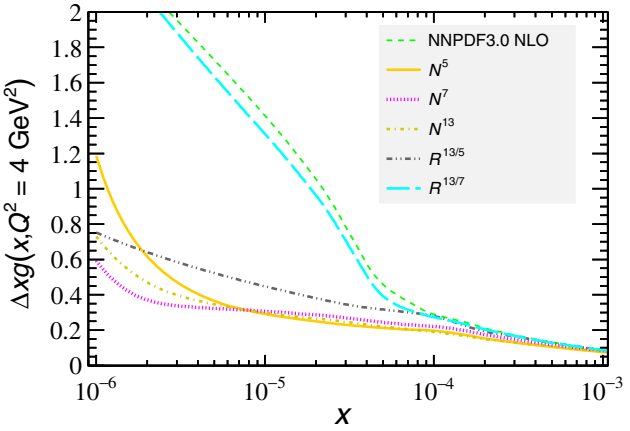

FIG. 1. The 1σ relative PDF uncertainties for the small-x gluon at $Q^2 = 4\ \mathrm{GeV}^2$ in NNPDF3.0 and in the subsequent fits when the LHCb charm data are included one at a time.

consistent for all three combinations, down to $x \simeq 10^{-6}$, and, as expected from Fig. 1, we observe a dramatic reduction of the 1σ PDF uncertainties. We have verified that these updated results are consistent with our original study [Gauld, Rojo, Rottoli, and Talbert (GRRT)] [14], yet significantly more precise; see Fig. 5.

Given the sizable theory errors that affect charm production, it is important to assess the robustness of our results with respect to the scale variations of the NLO calculation as well as to the value of m_c. We thus have quantified how the resultant gluon are affected by theory variations, including $\mu = \sqrt{4m_c^2 + p_T^2}$, alternative reference bins $y_{\mathrm{ref}}^{D^0} = [2.5, 3.0]$ and [3.5, 4.0], and charm mass variations of $\Delta m_c = 0.2$ GeV. The resultant central values of the gluon are shown in Figs. 3 and 4 in comparison to NNPDF3.0 and to the 1σ PDF uncertainty band from the $N_5 + N_7 + N_{13}$ and $N_7 + R_{13/5}$ fits, respectively.

We find that our results are reasonably stable upon these variations of the input theory settings, particularly for the

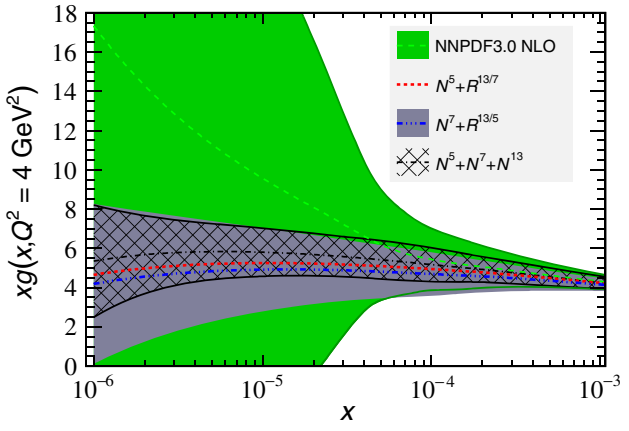

FIG. 2. The NLO gluon in NNPDF3.0 and for various combinations of the included LHCb data, at $Q^2 = 4\ \mathrm{GeV}^2$.

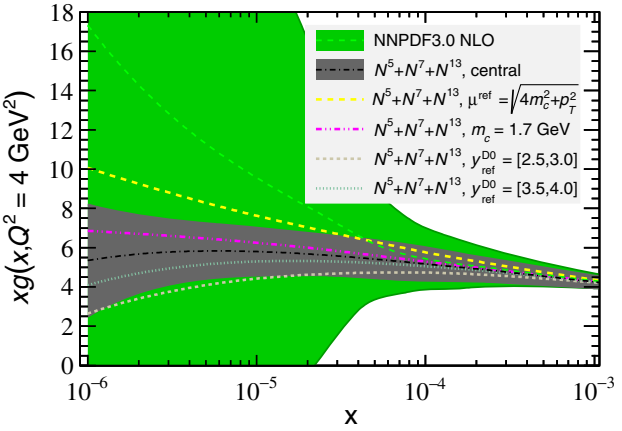

FIG. 3. Dependence of the small-x gluon from the $N_5 + N_7 + N_{13}$ fits for variations in the input theory settings.

$N^7 + R^{13/5}$ fits, highlighting that the cancellation of theory errors is more effective for the cross-section ratios than for the normalized distributions. Even for the most constraining combination, the $N_5 + N_7 + N_{13}$ fits, all of the theory variations are contained within the 95% confidence level interval of the PDF uncertainty. This study demonstrates that the sizable reduction of the small-x gluon PDF errors is robust with respect to theoretical uncertainties. A further reduction of the scale dependence could only be achieved with the full NNLO calculation.

Our precision determination of the small-x gluon has important phenomenological implications, which we choose to illustrate with two representative examples: the longitudinal structure function F_L at a future high-energy lepton-proton collider and the UHE neutrino-nucleus cross section. First, we have computed $F_L(x, Q^2)$ for $Q^2 = 3.5\ \mathrm{GeV}^2$ using APFEL [40] in the FONLL-B general mass scheme [41]. The proposed Large Hadron Electron Collider (LHeC) would be able to measure F_L down to $x \gtrsim 10^{-6}$ with a few percent precision for $Q^2 \gtrsim 2\ \mathrm{GeV}^2$ [10], hence providing a unique probe of Balitsky-Fadin-Kuraev-Lipatov resummations and nonlinear QCD dynamics [42].

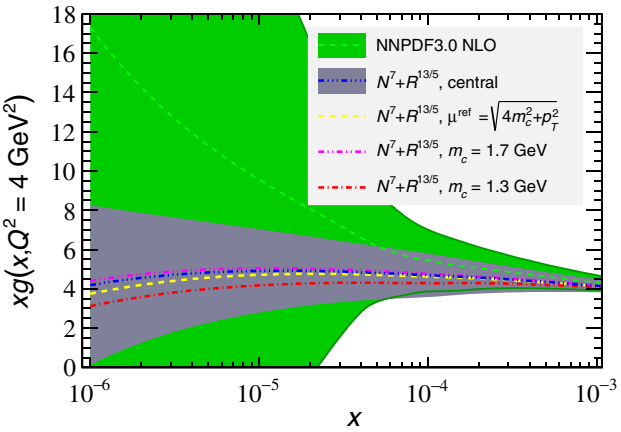

FIG. 4. Same as Fig. 3 for the $N^7 + R^{13/5}$ fits.

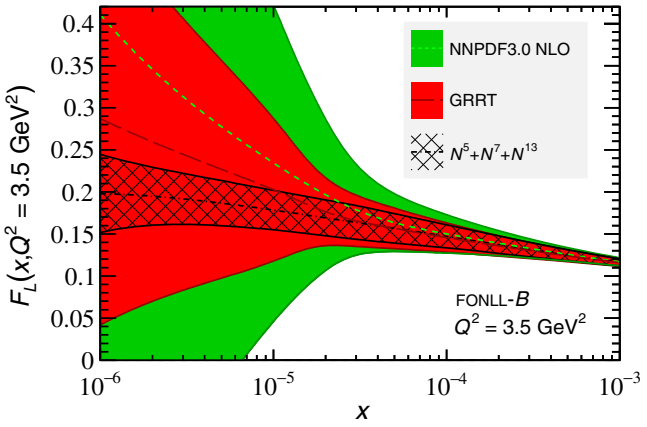

FIG. 5. The structure function $F_L(x, Q^2)$ at $Q^2 = 3.5$ GeV^2, comparing the NNPDF3.0 predictions both with the results of this work and with the GRRT calculation.

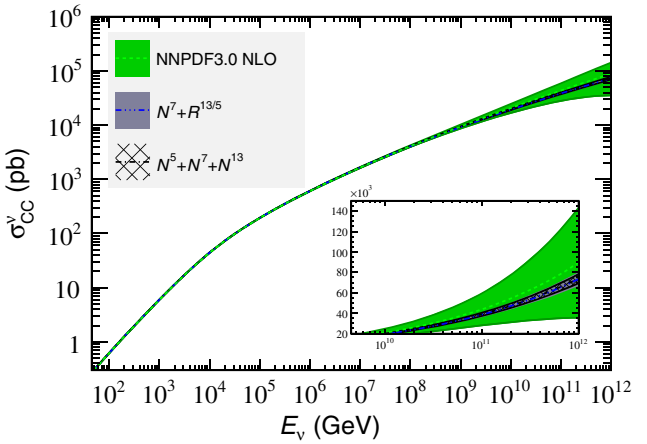

FIG. 6. The NLO charged-current neutrino-nucleus cross section as a function of the neutrino energy E_ν, computed with NNPDF3.0 and with the results of this work.

In Fig. 5, we compare F_L computed with NNPDF3.0and with the results of this work, as well as with the original GRRT calculation. We observe that the PDF uncertainties on F_L at $x \simeq 10^{-6}$ are now reduced by around a factor of 7 with respect to the baseline, and that F_L itself is always positive for the x range accessible at the LHeC.

Next, we have computed the UHE charged-current (CC) neutrino-nucleus cross section as a function of the incoming neutrino energy E_ν, using a stand-alone code based on APFEL for the calculation of the NLO structure functions. At the highest values of E_ν that might be accessible at neutrino telescopes such as IceCube [43] and KM3NET [44], the neutrino-nucleus interactions probe the quark sea PDFs at $Q^2 \simeq M_W^2$ and down to $x \simeq 10^{-8}$, a region where the quark distributions are driven by the small-x gluon by means of Dokshitzer-Gribov-Lipatov-Altarelli-Parisi evolution effects [45].

In Fig. 6, we compare the CC UHE neutrino-nucleus cross section from NNPDF3.0 with the results of this work. As in the case of F_L, we find a sizable reduction of the PDF uncertainties, which represent, by far, the dominant theory uncertainty for this process at high E_ν. This way, NLO QCD provides a prediction accurate to $\lesssim$10% up to $E_\nu \simeq 10^{12}$ GeV, a region where a rather different behavior is found in scenarios with nonlinear QCD evolution effects [46]. Our results for the UHE cross section are more precise than the existing calculations [47], based on PDF fits where the only constraints on the small-x gluon come from the inclusive and charm HERA data, and they therefore provide a clean handle for disentangling possible beyond the standard model effects in this process [48].

To summarize, in this Letter, we have presented a precision determination of the small-x gluon down to $x \simeq 10^{-6}$ from LHCb charm production in the forward region at $\sqrt{s} = 5, 7$, and 13 TeV. We have shown that the LHCb data provided at the three c.m. energies leads to consistent constraints on the small-x gluon, and we have determined the combination that maximizes the reduction of PDF uncertainties, namely, the sum of normalized distributions $N^5 + N^7 + N^{13}$. We have found indications that NLO QCD may not be adequate to describe the most precise data, a subset of points for the D^0 final state at 5 and 13 TeV (here excluded by kinematical cuts), suggesting that NNLO corrections are required to exploit the full LHCb charm data set. Our analysis provides a strong motivation for including the LHCb charm production data in the next generation of global PDF fits, such as the upcoming NNPDF3.1 release.

We have illustrated how the improved small-x gluon will lead to significantly reduced theory uncertainties for F_L at future high-energy lepton-proton colliders and for the UHE neutrino-nucleus interactions. We have, however, only scratched the surface of the phenomenological implications of our work. It is important to explore these implications further to inform other applications, such as the modeling of semihard QCD processes at the LHC in Monte Carlo event generators and for calculations of cosmic ray production. Moreover, it would be interesting to compare our determination of the small-x gluon with those that could be achieved from other processes with similar kinematical coverage, such as exclusive production [49] or forward photon production [50,51].

The results of this work are available upon request in the form of LHAPDF6 grids [35].

We thank L. Rottoli and V. Bertone for the calculations of the UHE neutrino cross sections and for assistance with APFEL. We are also grateful to Dominik Müller and Alex Pearce for information with regards to the LHCb data. We acknowledge the support provided by the GridPP Collaboration. The work of J. R. is partially supported by the ERC Starting Grant "PDF4BSM." The work of R. G. is supported by the ERC Advanced Grant MC@NNLO (No. 340983).

*rgauld@phys.ethz.ch
†j.rojo@vu.nl

[1] S. Forte and G. Watt, Annu. Rev. Nucl. Part. Sci. **63**, 291 (2013).
[2] J. Butterworth *et al.*, J. Phys. G **43**, 023001 (2016).
[3] J. Rojo *et al.*, J. Phys. G **42**, 103103 (2015).
[4] P. Skands, S. Carrazza, and J. Rojo, Eur. Phys. J. C **74**, 3024 (2014).
[5] A. Cooper-Sarkar, P. Mertsch, and S. Sarkar, J. High Energy Phys. 08 (2011) 042.
[6] M. V. Garzelli, S. Moch, and G. Sigl, J. High Energy Phys. 10 (2015) 115.
[7] R. Gauld, J. Rojo, L. Rottoli, S. Sarkar, and J. Talbert, J. High Energy Phys. 02 (2016) 130.
[8] A. Bhattacharya, R. Enberg, Y. S. Jeong, C. S. Kim, M. H. Reno, I. Sarcevic, and A. Stasto, J. High Energy Phys. 11 (2016) 167.
[9] D. d'Enterria, R. Engel, T. Pierog, S. Ostapchenko, and K. Werner, Astropart. Phys. **35**, 98 (2011).
[10] J. Abelleira Fernandez *et al.* (LHeC Study Group), J. Phys. G **39**, 075001 (2012).
[11] M. L. Mangano *et al.*, arXiv:1607.01831.
[12] H. Abramowicz *et al.* (H1 and ZEUS Collaborations), Eur. Phys. J. C **73**, 2311 (2013).
[13] H. Abramowicz *et al.* (ZEUS and H1 Collaborations), Eur. Phys. J. C **75**, 580 (2015).
[14] R. Gauld, J. Rojo, L. Rottoli, and J. Talbert, J. High Energy Phys. 11 (2015) 009.
[15] O. Zenaiev *et al.* (PROSA Collaboration), Eur. Phys. J. C **75**, 396 (2015).
[16] M. Cacciari, M. L. Mangano, and P. Nason, Eur. Phys. J. C **75**, 610 (2015).
[17] R. Aaij *et al.* (LHCb Collaboration), Nucl. Phys. **B871**, 1 (2013).
[18] M. L. Mangano and J. Rojo, J. High Energy Phys. 08 (2012) 010.
[19] R. Aaij *et al.* (LHCb Collaboration), arXiv:1610.02230.
[20] R. Aaij *et al.* (LHCb Collaboration), J. High Energy Phys. 03 (2016) 159; 09 (2016) 013(E).
[21] The LHCb 13 TeV data considered here account for a recently released erratum [20] which primarily affected low-p_T D^0 data.
[22] R. D. Ball *et al.* (NNPDF Collaboration), J. High Energy Phys. 04 (2015) 040.
[23] M. Cacciari and M. Greco, Nucl. Phys. **B421**, 530 (1994).
[24] P. Nason, J. High Energy Phys. 11 (2004) 040.
[25] S. Frixione, P. Nason, and C. Oleari, J. High Energy Phys. 11 (2007) 070.
[26] S. Alioli, P. Nason, C. Oleari, and E. Re, J. High Energy Phys. 06 (2010) 043.
[27] S. Frixione, P. Nason, and G. Ridolfi, J. High Energy Phys. 09 (2007) 126.
[28] T. Sjostrand, S. Mrenna, and P. Z. Skands, Comput. Phys. Commun. **178**, 852 (2008).
[29] T. Sjöstrand, S. Ask, J. R. Christiansen, R. Corke, N. Desai, P. Ilten, S. Mrenna, S. Prestel, C. O. Rasmussen, and P. Z. Skands, Comput. Phys. Commun. **191**, 159 (2015).
[30] M. Cacciari, S. Frixione, N. Houdeau, M. L. Mangano, P. Nason, and G. Ridolfi, J. High Energy Phys. 10 (2012) 137.
[31] S. Frixione and B. R. Webber, J. High Energy Phys. 06 (2002) 029.
[32] J. Alwall, R. Frederix, S. Frixione, V. Hirschi, F. Maltoni, O. Mattelaer, H.-S. Shao, T. Stelzer, P. Torrielli, and M. Zaro, J. High Energy Phys. 07 (2014) 079.
[33] M. Cacciari, M. Greco, and P. Nason, J. High Energy Phys. 05 (1998) 007.
[34] M. Cacciari, S. Frixione, and P. Nason, J. High Energy Phys. 03 (2001) 006.
[35] A. Buckley, J. Ferrando, S. Lloyd, K. Nordström, B. Page, M. Rüfenacht, M. Schönherr, and G. Watt, Eur. Phys. J. C **75**, 132 (2015).
[36] D. de Florian *et al.* (LHC Higgs Cross Section Working Group), arXiv:1610.07922.
[37] R. D. Ball, V. Bertone, F. Cerutti, L. Del Debbio, S. Forte, A. Guffanti, J. I. Latorre, J. Rojo, and M. Ubiali (NNPDF Collaboration), Nucl. Phys. **B849**, 112 (2011).
[38] R. D. Ball, V. Bertone, F. Cerutti, L. Del Debbio, S. Forte, A. Guffanti, N. P. Hartland, J. I. Latorre, J. Rojo, and M. Ubiali, Nucl. Phys. **B855**, 608 (2012).
[39] M. Czakon, P. Fiedler, D. Heymes, and A. Mitov, J. High Energy Phys. 05 (2016) 034.
[40] V. Bertone, S. Carrazza, and J. Rojo, Comput. Phys. Commun. **185**, 1647 (2014).
[41] S. Forte, E. Laenen, P. Nason, and J. Rojo, Nucl. Phys. **B834**, 116 (2010).
[42] J. Rojo and F. Caola, arXiv:0906.2079.
[43] M. G. Aartsen *et al.* (IceCube Collaboration), Phys. Rev. Lett. **117**, 241101 (2016).
[44] S. Adrián-Martínez *et al.* (KM3Net Collaboration), J. Phys. G **43**, 084001 (2016).
[45] R. D. Ball and S. Forte, Phys. Lett. B **335**, 77 (1994).
[46] J. L. Albacete, J. I. Illana, and A. Soto-Ontoso, Phys. Rev. D **92**, 014027 (2015).
[47] A. Connolly, R. S. Thorne, and D. Waters, Phys. Rev. D **83**, 113009 (2011).
[48] L. A. Anchordoqui *et al.*, J. High Energy Astrophys. **1–2**, 1 (2014).
[49] S. P. Jones, A. D. Martin, M. G. Ryskin, and T. Teubner, Eur. Phys. J. C **76**, 633 (2016).
[50] D. d'Enterria and J. Rojo, Nucl. Phys. **B860**, 311 (2012).
[51] T. Peitzmann (for the ALICE FoCal Collaboration), *Proc. Sci.* DIS2016 (2016) 273 [arXiv:1607.01673].